Proceedings of the 2005 IEEE
International Conference on Robotics and Automation
Barcelona, Spain, April 2005

Circular/Spherical Robots for Crawling and Jumping

Yuuta Sugiyama, Ayumi Shiotsu, Masashi Yamanaka, and Shinichi Hirai
Dept. Robotics, Ritsumeikan Univ.
Kusatsu, Shiga 525-8577, Japan
http://www.ritsumei.ac.jp/se/˜hirai/

***Abstract*— We describe circular/spherical robots for crawling and jumping. Locomotion over rough terrain has been achieved mainly by rigid body systems including crawlers and leg mechanisms. This paper presents an alternative method of moving over rough terrain, one that employs deformation. First, we describe the principle of crawling and jumping as performed through deformation of a robot body. Second, in a physical simulation, we investigate the feasibility of the approach. Next, we show experimentally that prototypes of a circular robot and a spherical robot can crawl and jump.**

***Index Terms*— deformation, locomotion, crawling, jumping, soft body.**

I. Introduction

Rough terrain locomotion has mainly relied on rigid body systems, such as crawlers and leg mechanisms. This paper presents an alternative approach that uses deformation.

Locomotion mechanisms consisting of rigid body systems have drawbacks: large weight that may cause impact to humans and difficulty in recovery from their overturning. Recently, mechanisms that can recover from their overturning have been studied [1], [2], but these mechanisms tend to be complicated. An alternative approach to light-weighted and simple mechanisms is thus required. Recent researches on soft actuators such as shape memory alloy (SMA) wires and polymer gel actuators has yielded impressive results [3], [4], [5]. Soft actuators have been used to drive leg mechanisms and soft body robots [6]. Locomotion mechanisms consisting of soft actuators can be light-weighted. Unfortunately, soft actuators still have drawbacks. They tend to generate a small force, and those that generate a large force need either a high driving voltage over 1,000V, making it difficult to build self-supporting robots, or a wet environment. To overcome this problem, we employ soft actuators to controllably deform a robot body, enabling it to crawl over and jump on rough terrain. Crawling and jumping using deformation can cope with rougher terrain than rigid body systems can. Additionally, soft body deformation reduces the damage in collision with humans.

In this paper, we propose a circular robot and a spherical robot and describe their performance in a simulation and in a practical experiment. First, we briefly explain the principle of crawling and jumping as performed through deformation of a robot body. Second, in a physical simulation, we investigate the feasibility of the approach. Next, we show experimentally that prototypes of a circular robot and a spherical robot can crawl and jump.

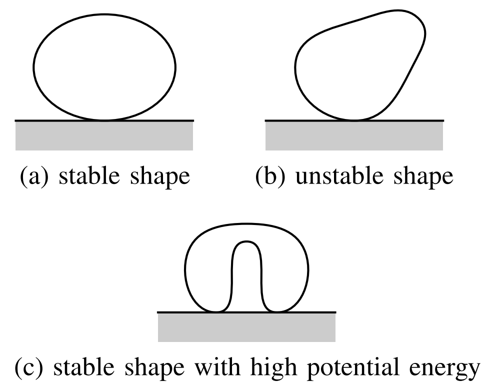

Fig. 1. Principle of crawling and jumping

II. Principle of Crawling and Jumping by Deformation

Suppose a robot is in stable on the ground, as illustrated in Figure 1-(a). Then, the gravitational potential energy of the robot reaches to its minimum; implying that the gradient of the energy is equal to zero. Self-deformation of the robot body changes the gradient of the gravitational potential energy; it generates a moment by a gravitational force around the area the robot is in contact with the ground. The moment causes the robot to move on the ground. If the robot deforms from a stable shape into an unstable shape described in Figure 1-(b), it rotates clockwise and moves towards the right. Successive deformation of the robot body, which can be generated by actuators, enables a continuous crawling motion along the ground. Consequently, the proposed approach for crawling uses the change of the gravitational potential energy caused by its deformation.

Deformation allows elastic potential energy to be stored which, if released rapidly enough, can generate a force large enough to make the robot jump. Now suppose the robot deforms from one stable shape into another, which has high potential energy as illustrated in Figure 1-(c). If the potential energy is released rapidly enough, the robot will jump. The high-energy shape shown in Figure 1-(c) turns, with a small disturbance, into the stable shape shown in Figure 1-(a), generating the force required for the jump. Consequently, the proposed approach for jumping uses the charge and release of elastic potential energy. Actuators inside the robot body can be used to store this elastic energy. The forces required to store the elastic energy is generally much smaller than those required to perform a jump. Such charge and release of elastic energy can be found in the jump of insects [7].

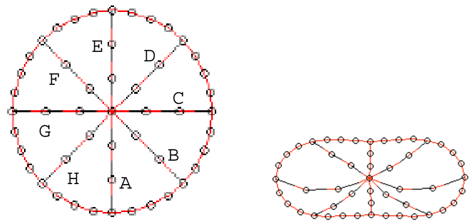

(a) initial shape (b) deformed shape

Fig. 2. Circular soft robot

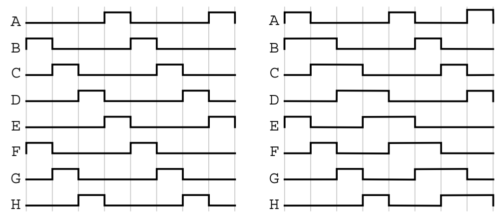

(a) pattern BF (b) pattern ABE

Fig. 3. Voltage patterns applied to SMA coils

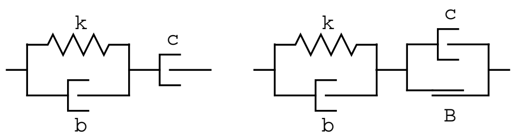

(a) three-element model (b) three-element model with slider

Fig. 4. Model of SMA coils

III. Feasibility Investigation through Physical Simulation

In this section, in a physical simulation, we assess the feasibility of a deformable robot to crawl and jump.

A. Modeling of circular soft robot

Let us simulate the behavior of the circular soft robot illustrated in Figure 2. The circular soft robot consists of a circular elastic shell with a set of soft actuators inside, as shown in Figure 2-(a). The robot has eight SMA coils labelled as A through H. Extending or shrinking actuators deforms the robot body, i.e., the circular shell, as shown in Figure 2-(b). We apply open-loop PWM control to the coils. A periodic voltage pattern is applied to the set of SMA coils during crawling. As illustrated in Figure 3, periodic voltage patterns are denoted by the set of coils active during the first time step. Figure 3-(a) illustrates pattern BF, where SMA coils B and F are activated during the first time step, coils C and G during the second time step, coils D and H during the third time step, and so on. Figure 3-(b) illustrates pattern ABE, where SMA coils A, B, and E are activated during the first time step and coils B, C, and F during the next time step.

The elastic shell of the robot is modeled as a viscoelastic object while actuators are modeled as rheological objects [8], so as to be able to describe the inelastic nature of the SMA coils and polymer gel actuators. We can specify

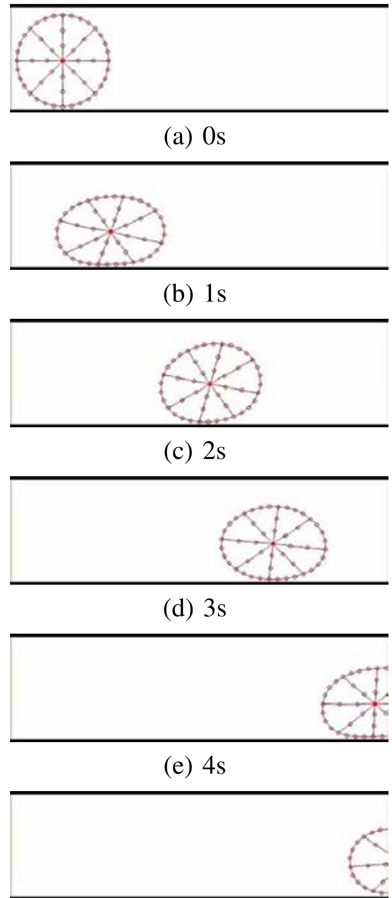

(a) 0s (b) 1s (c) 2s (d) 3s (e) 4s (f) 5s

Fig. 5. Simulation of a circular soft robot crawling

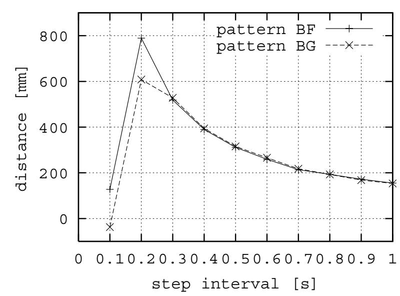

Fig. 6. Comparison of pattern BF and BG

the contraction rate, maximum contraction, and maximum generated force of an SMA coil using a three-element model with a slider.

The extension of an elastic shell is described by a Voigt model, while its bend is modeled as an elastic element. The Voigt model for extension is a parallel connection of an elastic element k_{body} and a viscous element b_{body}. The elastic element for bend deformation is denoted as k_{bend}. We have experimentally identified model parameters for the elastic shell of a prototype of a circular soft robot in advance: k_{body} = 500N/m, b_{body} = 0.1N/(m/s), and k_{bend} = 0.0015Nm/rad.

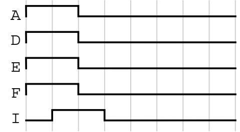

Fig. 7. Voltage patterns for jumping

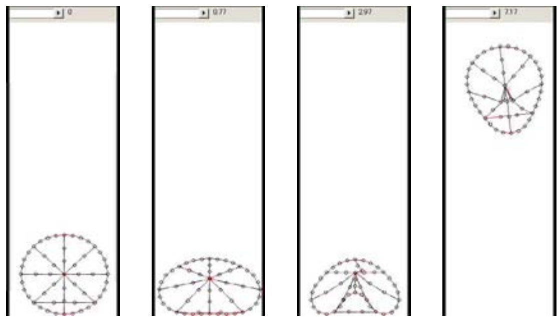

(a) 0s (b) 2s (c) 4s (d) 9s

Fig. 8. Simulation of a circular soft robot jumping

B. Modeling of SMA coil

Let us first formulate the passive deformation of an SMA coil that deforms in response to an applied external force. SMA coils show both viscoelastic and plastic deformation properties, which suggests their deformation can be modeled by a three-element model. A three-element model is a serial connection of a Voigt element and a viscous element, as illustrated in Figure 4-(a). The elastic coefficient k and damping coefficient b specify the Voigt element, while the viscous coefficient c characterizes the viscous element. Let x be the length of a three-element model. Let x_v and x_d be the lengths of a Voigt model and a viscous element, respectively. The three-element model can be formulated as follows:

$$x = x_v + x_d, \tag{1}$$

$$f_{pas} = -k(x_v - x_v^{\mathrm{init}}) - b\dot{x}_v, \tag{2}$$

$$f_{pas} = -c\dot{x}_d \tag{3}$$

where f_{pas} describes a passive force generated by the element and x_v^{init} is the initial length of the Voigt model in the element.

A three-element model can extend as long as an external force is applied to it. To avoid such limitless extension, we employ a three-element model with a slider illustrated in Figure 4-(b). The slider is specified by force limit B. In a three-element model with a slider, eq.(3) is replaced by the following equation:

$$-c\dot{x}_d = \begin{cases} f_{pas} & \text{if } \ fx \leq Bx_v^{\mathrm{init}} \\ 0 & \text{otherwise} \end{cases} \tag{4}$$

where f stands for the resultant external force applied to the element.

An SMA coil actively generates a force that is determined by the voltage applied to it. Let us next formulate this actively generated force. Let $V(t)$ be the voltage applied to a coil. We apply open-loop PWM to the generation of a force by a coil. That is, voltage $V(t)$ alternates between V or 0. Let $F(t)$ be a force actively generated by an SMA coil at time t. Let D_{on} be the contraction force rate of the coil and D_{off} its relaxation force rate. Let F_{max} be the maximum force that can be generated by the coil. The force generated by the SMA coil can then be expressed as:

$$\frac{\mathrm{d}F}{\mathrm{d}t} = \begin{cases} D_{on} & V(t) = V \ \text{ and } \ F(t) < F_{max} \\ -D_{off} & V(t) = 0 \ \text{ and } \ F(t) > 0 \\ 0 & \text{otherwise} \end{cases} . \tag{5}$$

Integration of the above equation over the time interval $[0, t]$ yields the actively generated force at time t. Note that force $F(t)$ varies in the range $[0, F_{max}]$.

We have used SMA coils BMX100 to build a prototype of a circular soft robot. We have experimentally identified the model parameters to be used in eqs.(1)-(5): $k = 50$N/m, $b = 0.1$N/(m/s), $c = 10$N/(m/s), $B = 0.016$N, $D_{on} = D_{off} = 150$mN/s, and $F_{max} = 150$mN.

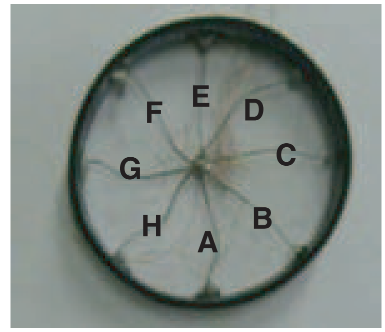

Fig. 9. Prototype of a circular soft robot

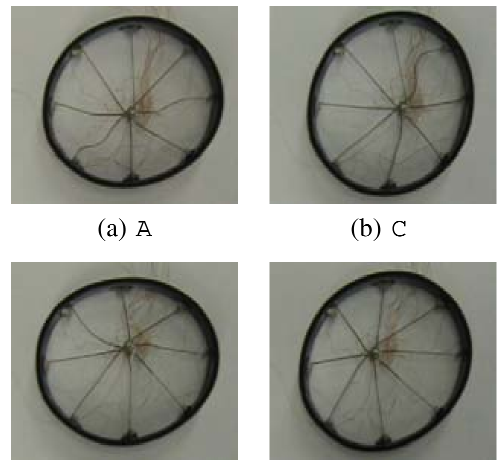

(a) A (b) C

(c) E (d) G

Fig. 10. Deformation of a circular soft robot

C. Simulation results

Figure 5 shows the simulation results of the crawling of a circular soft robot. A periodic voltage pattern is applied to one or more of the SMA coils during the crawl. In this simulation, pattern BF illustrated in Figure 3-(a) was used to activate the coils. The figure shows that a circular robot can crawl on a flat terrain by open-loop PWM control of eight SMA coils. In addition, we can find

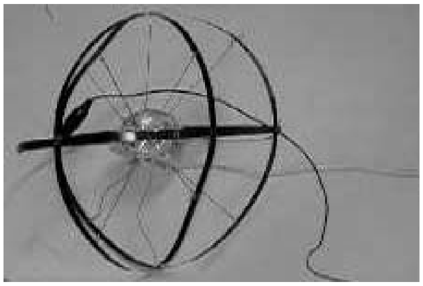

Fig. 11. Prototype of a spherical soft robot

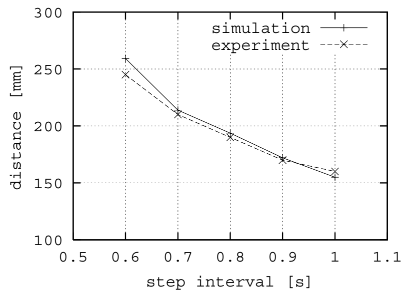

Fig. 13. Comparison between simulation and experimental results for voltage pattern BF

an appropriate voltage pattern through simulation. Figure 6 shows locomotion distances covered over 10s at various step intervals. As shown in the figure, voltage pattern BF with a step interval of 0.2s yields the better result.

We have attached an SMA coil labelled as I between the end points of B and H on the circular shell for jumping in addition to the eight SMA coils. Voltage pattern illustrated in Figure 7 is applied to a set of SMA coils. Four SMA coils A, D, E, and F are activated before activating coil I. The four coils are then released before releasing coil I. Figure 8 shows the simulation results for a jump performed by a circular soft robot. The results suggest that the robot can jump under gravity through PWM control of coils.

We can simulate the 3D motion of a spherical robot using the proposed modeling methods.

IV. Experimental Results

We build two prototypes of a soft robot, a circular soft robot and a spherical soft robot, to assess experimentally the feasibility of a deformable robot crawling and jumping. A prototype of a circular soft robot is shown in Figure 9, which consists of eight BMX100 SMA coils, labelled A through H, attached to the inside of a circular rubber shell. The diameter of the circular body is 40mm and the robot weighs 3g. When voltage is applied to a coil, it contracts, resulting in the circular rubber deforming as shown in Figure 10. Each figure corresponds to the deformation caused by the contraction of an individual coil A, C, E, and G. A prototype of a spherical soft robot is shown in Figure 11, which consists of 18 BMX SMA coils. The diameter of the spherical body is 200mm and the robot weights 137g. A driving circuit for SMA coils of weight 75g is attached inside the spherical body.

Fig. 17. Spherical prototype for crawling and jumping

A. Crawling

Figure 12 shows a sequence of snapshots of the circular prototype crawling. Voltage pattern BF is applied to SMA coils. As shown in the figure, the circular robot can crawl on a flat ground. Let us compare the simulation and experimental results for crawling. Figure 13 describes locomotion distances covered over 10s at various step intervals. The prototype moves 260mm over 10s at a step interval of 0.6s. Namely, the prototype moves in average about 65% of its diameter per second. As shown in the figure, simulation results agree with experimental results. Reducing the step interval within a certain range results in faster locomotion. Note that an activated SMA coil extends back to its natural length via natural radiation of heat, which limits the locomotion speed.

Figure 14 shows a sequence of snapshots of the spherical prototype crawling. As shown in the figure, the spherical robot can crawl on a flat ground.

B. Slope-climbing

Figure 15 shows a sequence of snapshots of the prototype climbing a slope. The prototype can climb up a slope of 20° by applying pattern ABE illustrated in Figure 3-(b).

C. Jumping

Recall that an SMA coil I is activated for jumping of a circular prototype, as described in Section III-C. Figure 16 shows a sequence of snapshots of the circular prototype jumping. The prototype can jump a distance of 80mm, which is twice its diameter.

Spherical prototype shown in Figure 11 cannot jump. Thus, we have built another spherical prototype for jumping shown in Figure 17. The prototype consists of 18 SMA coils for crawling and 4 SMA coils for jumping. The driving circuit is outside of the body to reduce the weight of the robot. The diameter of the spherical body is 90mm and the robot weights 5g. Figure 18 shows a sequence of snapshots of the spherical prototype jumping. The prototype can jump a distance of 200mm, which is twice its diameter.

V. Concluding Remarks

In the present study, we proposed a deformable robot capable of crawling and jumping. First, we described the principle of crawling and jumping using the deformation of a robot body. Second, in a physical simulation using a three-element model with a slider, we showed the feasibility of the robot to crawl and jump. Finally, we

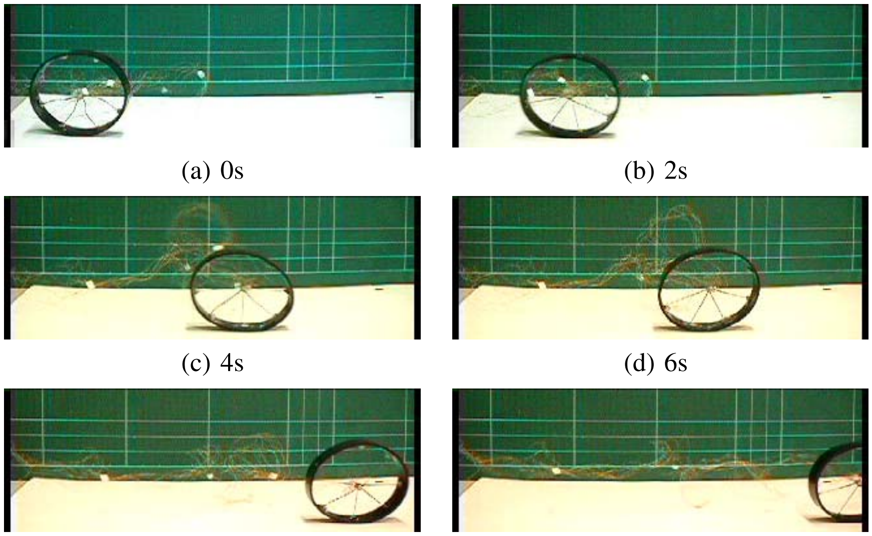

(a) 0s (b) 2s
(c) 4s (d) 6s
(e) 8s (f) 10s

Fig. 12. Circular soft robot crawling

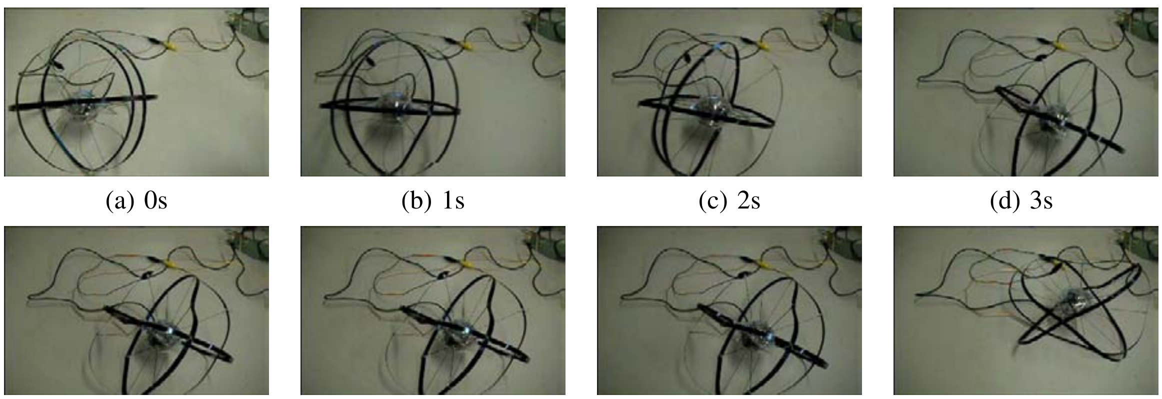

(a) 0s (b) 1s (c) 2s (d) 3s
(e) 4s (f) 5s (g) 8s (h) 16s

Fig. 14. Spherical soft robot crawling

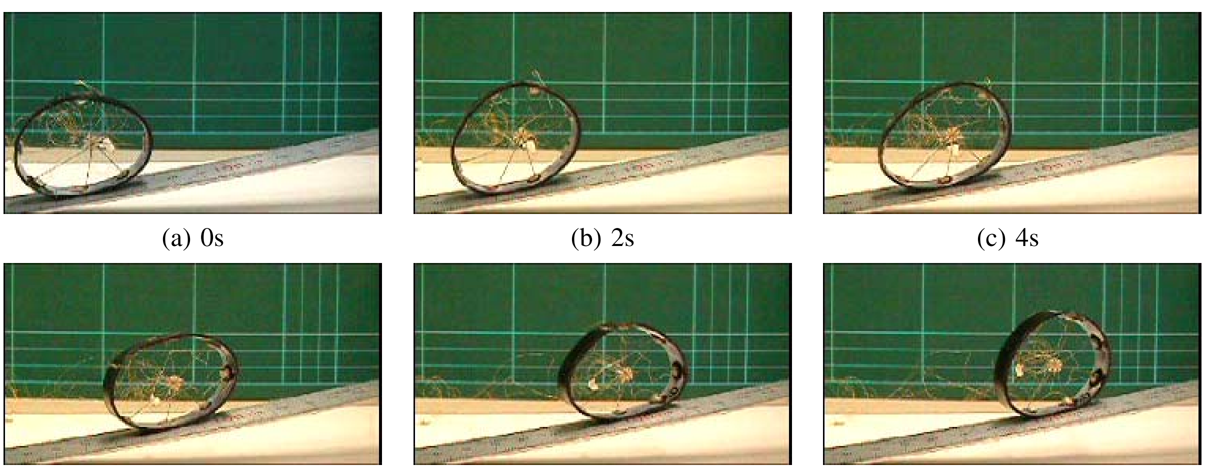

(a) 0s (b) 2s (c) 4s
(f) 8s (e) 12s (f) 16s

Fig. 15. Circular soft robot climbing a slope

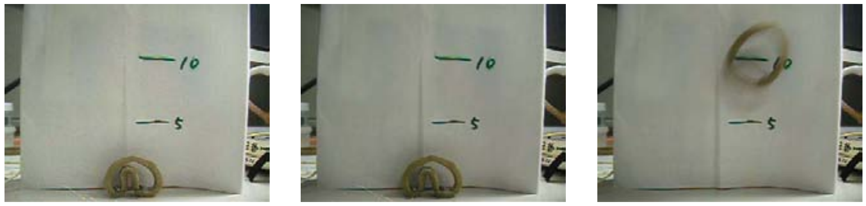

(a) 0s (b) 4s (d) 6s

Fig. 16. Circular soft robot jumping

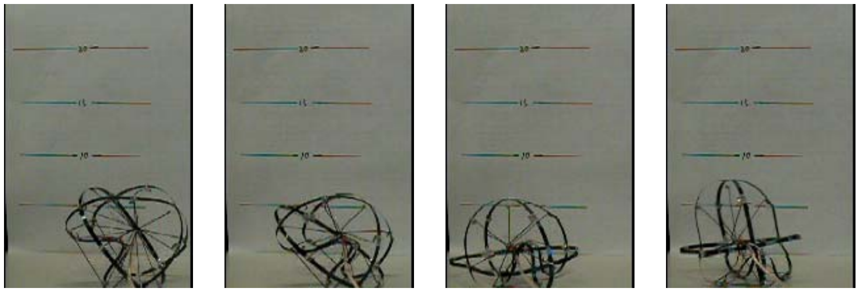

(a) 0s (b) 4s (c) 8s (d) 16s

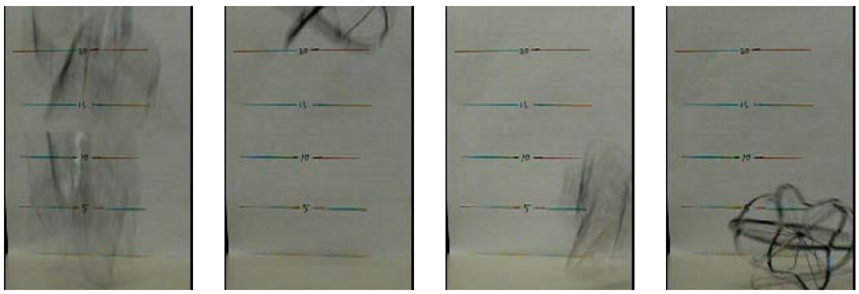

(e) 16s (f) 17s (g) 17s (h) 18s

Fig. 18. Spherical soft robot jumping

experimentally verified that prototypes of a circular soft robot and a spherical soft robot can crawl and jump. The circular prototype moves about 65% of its diameter per second, climbs up a slope of 20°, and jump twice its diameter.

To date, no analysis has been conducted on the motion of a circular robot and a spherical robot. In further studies, we will apply linear object modeling [9] to analyze and optimize the motion of a circular robot. We will evaluate the potential energy of a circular soft robot during crawling and jumping in order to get a better understanding of the system. We have built a prototype of a spherical soft robot but its performance has been little evaluated. We evaluate the performance of a spherical prototype to compare its experimental and simulation results. No sensor feedback has been introduced to a deformable soft robot. Orientation control using an accelerometer or a vision sensor is investigated for autonomous locomotion of a deformable soft robot.

Acknowledgement

This research was supported in part by the NEDO 21st Century Robot Challenge Program to demonstrate the prototypes in Aichi Expo 2005.

References

[1] Saranli, U., Buehler, M., and Koditschek, D. E., *RHex: A Simple and Highly Mobile Hexapod Robot*, Int. J. of Robotics Research, Vol. 20, No. 7, pp.616–631, 2001.

[2] Yim, M., Eldershaw, C., Zhang, Y., and Duff, D., *Limbless Conforming Gaits with Modular Robots*, Proc of Int. Symp. on Experimental Robotics, Singapore, June, 2004.

[3] Pelrine, R., Kornbluh, R., Pei, Q., and Joseph, J., *High-speed Electrically Actuated Elastomers with Strain Greater Than 100%*, Science, Vol. 287, February, pp.836–839, 2000.

[4] *The First Conference on Artificial Muscles*, December, 2001.

[5] *Artificial Muscles*, Scientific American, October, pp.34–41, 2003.

[6] Otake, M., Kagami, Y., Inaba, M., and Inoue, H., *Motion design of a starfish-shaped gel robots made of electroactive polymer gel*, Robotics and Autonomous Systems, Vol. 40, pp.185–191, 2002.

[7] Rothschild, M., Schlein, Y., and Ito, S., *A Colour Atlas of Insect Tissues via the Flea*, p.86, *The jumping flea*, Wolfe Publishing, 1986.

[8] Kimura, M., Sugiyama, Y., Tomokuni, S., and Hirai, S., *Constructing Rheologically Deformable Virtual Objects*, Proc. IEEE Int. Conf. on Robotics and Automation, Taipei, September, 2003.

[9] Wakamatsu, H. and Hirai, S., *Static Modeling of Linear Object Deformation based on Differential Geometry*, Int. J. Robotics Research, Vol. 23, No. 3, March, pp.293–311, 2004.